Regional Risk Assessment for climate change impacts on coastal aquifers

F. Iyalomhe [b], J. Rizzi [a,b], S. Pasini [a], S. Torresan [a], A. Critto [a,b], A. Marcomini [a,b,*]

[a] Centro Euro-Mediterraneo sui Cambiamenti Climatici (CMCC) via Augusto Imperatore 16, 73100 Lecce, Italy
[b] Department of Environmental Sciences, Informatics and Statistics, University Ca' Foscari Venice, Calle Larga S. Marta 2137, I-30123 Venice, Italy

HIGHLIGHTS

- The impact of climate change on the Esino River basin and groundwater is analyzed.
- Multi Criteria Decision Analysis is used to identify and rank areas/targets at risk.
- Salt water intrusion will affect a region close to the coastline.
- Risk maps allow a relevant assessment of risk levels guiding adaptation responses.

GRAPHICAL ABSTRACT
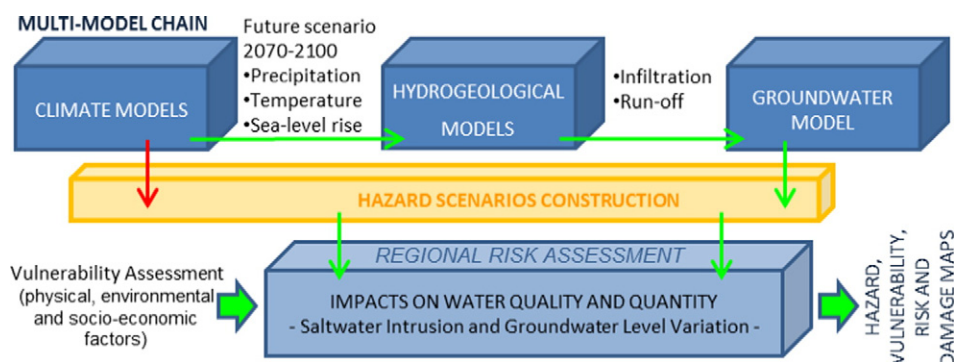
ABSTRACT

Coastal aquifers have been identified as particularly vulnerable to impacts on water quantity and quality due to the high density of socio-economic activities and human assets in coastal regions and to the projected rising sea levels, contributing to the process of saltwater intrusion. This paper proposes a Regional Risk Assessment (RRA) methodology integrated with a chain of numerical models to evaluate potential climate change-related impacts on coastal aquifers and linked natural and human systems (i.e., wells, river, agricultural areas, lakes, forests and semi-natural environments). The RRA methodology employs Multi Criteria Decision Analysis methods and Geographic Information Systems functionalities to integrate heterogeneous spatial data on hazard, susceptibility and risk for saltwater intrusion and groundwater level variation.

The proposed approach was applied on the Esino River basin (Italy) using future climate hazard scenarios based on a chain of climate, hydrological, hydraulic and groundwater system models running at different spatial scales. Models were forced with the IPCC SRES A1B emission scenario for the period 2071–2100 over four seasons (i.e., winter, spring, summer and autumn).

Results indicate that in future seasons, climate change will cause few impacts on the lower Esino River valley. Groundwater level decrease will have limited effects: agricultural areas, forests and semi-natural environments will be at risk only in a region close to the coastline which covers less than 5% of the total surface of the considered receptors; less than 3.5% of the wells will be exposed in the worst scenario. Saltwater intrusion impact in future scenarios will be restricted to a narrow region close to the coastline (only few hundred meters), and thus it is expected to have very limited effects on the Esino coastal aquifer with no consequences on the considered natural and human systems.

© 2015 Elsevier B.V. All rights reserved.

* Corresponding author at: University Ca' Foscari Venice, Department of Environmental Sciences, Informatics and Statistics, Dorsoduro, 2137, 30121 Venice Italy.
E-mail address: marcom@unive.it (A. Marcomini).

1. Introduction

Coastal groundwater resources connect the world's oceanic and hydrologic ecosystems (Moore, 1996; Ferguson and Gleeson, 2012) and play vital roles in the socio-economic and ecological functions of coastal systems worldwide (IPCC, 2007a). However, current research indicates that climate variability and climate change will constrain the usefulness of coastal groundwater through changes in climate variables (e.g., temperature, precipitation) and concomitant changes in the sea level (Sherif and Singh, 1999; Ranjan et al., 2006; Jyrkama and Sykes, 2007; Herrera-Pantoja and Hiscock, 2008; Ferguson and Gleeson, 2012; Bates et al., 2008). Thus, coastal groundwater-dependent natural and human systems (e.g., agricultural areas, natural systems, surface water bodies, etc.) will be prone to impacts related to changes in groundwater quantity and quality (Bates et al., 2008; Dragoni and Sukhija, 2008; Essink et al., 2010; Abd-Elhamid, 2010; Abd-Elhamid and Javadi, 2011). Moreover, according to several studies (e.g., Bates et al., 2008; Dragoni and Sukhija, 2008; Abd-Elhamid, 2010; Franssen, 2009; Baba et al., 2011; Praveena and Aris, 2010), climate change would bring impact on coastal groundwater directly, through the inter-action with surface water bodies, and indirectly, through the aquifers' recharge processes. But the extent to which these resources will be affected depends largely on the region's hydrogeological features and soil properties, and also on unsustainable human exploitation of aquifers and excessive use of soil (Herrera-Pantoja and Hiscock, 2008; Werner et al., 2012).

Several studies of coastal groundwater resources' interactions with climate change and anthropogenic pressures (e.g., Dentoni et al., 2014; Ferguson and Gleeson, 2012, Rasmussen et al., 2013, Franssen, 2009; Clarke et al., 2010, Re and Zuppi, 2011) revealed that these interactions would mostly affect coastal aquifers in the coastal arid and semi-arid re-gions, where groundwater shortage is already aggravated by recurrent droughts and by its excessive use for socio-economic activities (mainly in coastal communities, where half of the world's population lives and 8 of the 10 largest cities in the world are currently located) (Post, 2005; Carneiro et al., 2010).

Climate change interactions with global water resources, and partic-ularly with coastal groundwater aquifers, are well established, even though potential climate change effects at the regional scale are still un-certain. This is mainly due to the uncertainty related both to projections of climate variables (Baruffi et al., 2012) and the simulation of coastal aquifers' small-scale processes, such as spatial heterogeneities, geo-chemical reactions and hydrogeological changes that often demand detailed information about subsurface areas (Werner, 2010; Scibek and Allen, 2006). On numerous occasions this has resulted in poor re-search and understanding of the links between climate change and coastal groundwater resources, and its dependent natural and human systems.

As a result of these uncertainties, coastal groundwater resources' monitoring and investigation has been much discussed in recent studies both at the global scale (e.g., IPCC, 2007b; Barron et al., 2010; Werner, 2010) and at the regional scale (e.g., Bear et al., 1999, Holman, 2006; Herrera-Pantoja and Hiscock, 2008; Post and Abarca, 2010; Clarke et al., 2010; Essink et al., 2010; Gemitzi and Stefanopoulos, 2011; Barron et al., 2012; Dams et al., 2012), focusing on the assessment of climate change interactions with coastal groundwater resources through recharge and contamination pro-cesses. But none of these systematically considers the potential risk on coastal aquifer and on a variety of dependent natural and human systems. A few studies (e.g., Barron et al., 2012; Kløve et al., 2011) considered the effects of potential climate change on surface and groundwater dependent vegetation and also highlighted the need to evaluate hydro-ecological status and trends of groundwater-dependent ecosystems, but they did not actually assess and prioritize po-tential climate change risks for several dependent natural and human systems.

In view of this research gap, the present paper offers a comprehensive Regional Risk Assessment approach based on an ecosystem perspective (UNEP, 2009; http://www.cbd.int/ecosystem/) to adequately account for the complexity of coastal systems and their mutual interrelated impacts and to establish a causal link between identified stressors and possible receptors and areas (via ecological pathways). Accordingly, the paper proposes a spatially resolved Regional Risk Assessment (RRA) methodology that identifies all the necessary components involved in im-pact and risk analyses, including their possible relationship at the regional scale. It considers multiple habitats, multiple sources releasing a range of stressors that can impact multiple endpoints (Landis, 2005).

The spatially resolved methodology was based on the RRA conceptual framework (Fig. 1) applied within the European Life + SALT (Sustainable mAnagement of the Esino River basin to prevent saline intrusion in the coastaL aquifer in consideration of climaTe change, www.lifesalt.it) pro-ject, to analyze potential climate change impacts and risks on regional coastal groundwater resources in the Esino River basin (Italy). SALT was a pilot project intended to create a model for the implementation of two EU policy instruments: the Water Framework Directive (WFD; EC, 2000) and the Groundwater Directive, (EC, 2006). For this purpose, the spatially resolved RRA methodology developed within the Euro-Mediterranean Centre for Climate Change (CMCC, www.cmcc.it), was applied to evaluate potential groundwater quantity and quality related impacts on the Esino coastal aquifer and associated natural and human systems through the characterization of climate change hazard scenarios and the assessment of exposure, susceptibility, risks, and damages.

In the following sections, the case study area is introduced and the methodology is discussed through the application to the Esino River basin. Moreover, significant results related to exposure, susceptibility and risk maps produced for the defined climate change scenarios are analyzed in order to highlight areas and receptors at risk to climate-related impacts.

2. The case study area

The case study area is the lower Esino River valley (Fig. 2) that is extended for 137 km^2 and is part of the Esino River basin in the Marche region in central Italy. The Esino River basin has an extension of about 1203 km^2 and the Esino River length is about 86 km, from the Mount Cafaggio in the province of Macerata, to the municipality of Falconara Marittima, where it flows into the Adriatic Sea. The region's topography reveals two Apennines ridges: the Umbria–Marche ridge and the Marche ridge surrounding the Esino River valley. Moreover, the valley is generally steep-sided, narrow and deep with alluvial flood plains that extend wider eastward up to more than 10 km close to the Adriatic coast (Calderoni et al., 2007). Clays and marls define the region's geomorphology with millimetric silty–sandy layers from siliciclastic turbiditic synorogenic deposit (Alberti et al., 2009), often covered by alluvial deposits (from the Quaternary) to form the unconfined aquifer system. The region's al-luvial deposits increase in thickness from the inland toward the coast-line, due to previous Esino erosion action, and mainly comprise gravel, gravelly–sandy, and gravelly-clay with intercalated lenses of sand, clay and sandy silty clay (Coltori, 1997; Nanni, 1985; Alberti et al., 2009).

The climate varies from sub-continental along the coast in the north to temperate in the inland areas toward the south (with the seasonal variations in temperature). However, meteorological variables studied in the region of Jesi revealed that the average annual temperature is 14.4 °C and the cumulated precipitation is 827 mm/year (Bordi et al., 2001). This often resulted in torrential floods in the catchment during au-tumn and winter and a decreased flow during late spring and summer, with consequent strong influence on the environmental conditions.

The lower Esino River valley's location on the side of Adriatic coast makes it more vulnerable to potential impacts from natural and anthro-pogenic origin. In particular, the rapid growth in human population and urbanization within the Adriatic coastal area and the presence
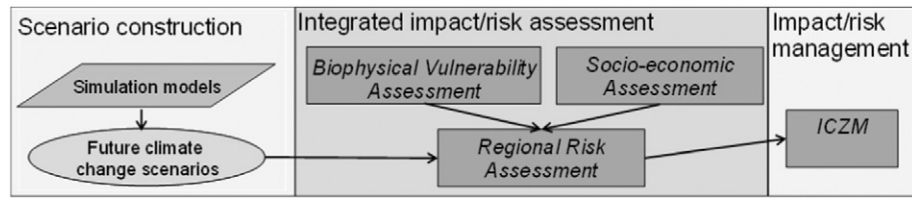
Fig. 1. RRA conceptual framework for the analysis of climate change impacts on coastal zone at the regional scale.

of hazardous plants and industrial infrastructures further accelerate its vulnerability. Moreover, the case study area is home to traditional agriculture for more than 100 km² (about 70% of the total surface) and few natural or semi-natural zones (i.e., 7 km², about 5% of the total surface), mainly located along the Esino riverbed. The demand for freshwater for agriculture, the unsustainable management of urban wastewater and the increased use of fertilizers in agriculture not only increases pressures on the region's confined and unconfined shallow aquifers but also impact groundwater quality and quantity (www.lifesalt.it/en/idea.html). Thus, the Esino wells and surface water supply network were affected by uncontrolled pollution loads untreated discharge and combined sewer overflows (Biondi and Baldoni, 1993; Biondi et al., 2003). Nevertheless, the request of freshwater for the population decreased from the mid 80s, reducing the pressure on the groundwater. In fact, all the municipalities have been progressively connected with a mountain aquifer that is characterized by a very high natural recharge rate allowing a sustainable exploitation of this source of drinkable water.

3. Materials and methods

The following sections present the model chain adopted within the LIFE + SALT project and the spatially resolved Regional Risk Assessment methodology applied to analyze potential effects of climate change on the Esino coastal aquifer and dependent natural and human systems.

3.1. The model chain

To simulate relevant climate, circulation, hydrological and hydrogeological processes that may influence climate change impacts on groundwater resources at different spatial scales, the model chain shown in Fig. 3 was applied to bridge the gap between large scale climate scenarios, often defined by global circulation models (GCM), and the fine scale scenarios where local impacts happen as a result of changed climate conditions. Accordingly, the proposed model chain includes climate, hydrological, hydraulic and groundwater models.
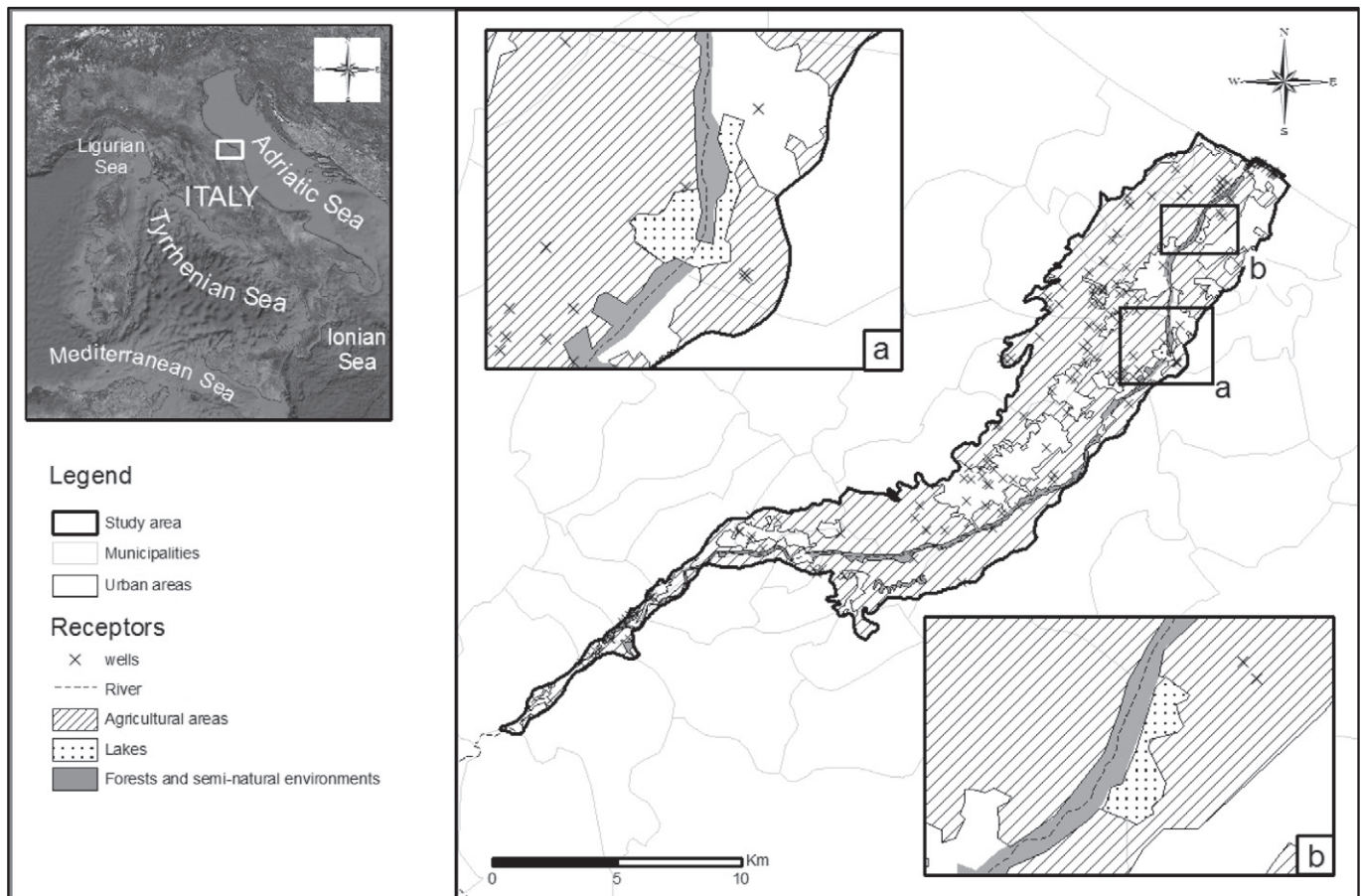

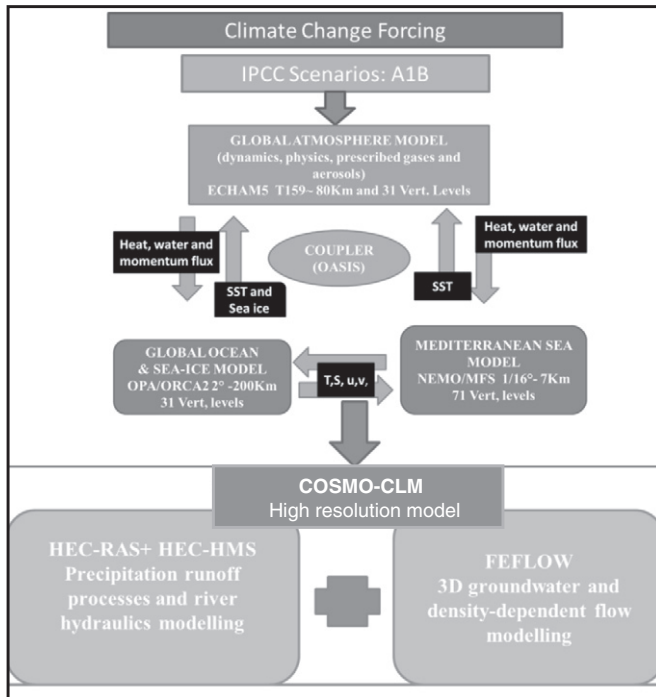**Fig. 2.** The case study area of the Esino River basin in Italy.

Fig. 3. The model chain defined within the SALT project. SST: Sea Surface Temperature; T: Temperature; S: Salinity; u: zonal velocity; v: meridional velocity.

The Global Ocean and Mediterranean Sea model (CMCC-MED), used to perform the entire Esino River basin's present and future climate projections, includes the coupled Atmosphere–Ocean Global Circulation Model (AOGCM) linked with a high-resolution Mediterranean Sea model (OPA/ORCA2 and NEMO/MFS). The AOGCM consists of a global atmosphere model (ECHAM5.4; Roeckner et al., 2003), with a horizontal resolution of about 80 km, and a global ocean model (OPA 8.2; Madec et al., 1998) with a horizontal resolution of about 2°, which includes the dynamic model of the sea ice LIM (Fichefet and Morales Maqueda, 1999). The Mediterranean Sea model is an interactive model implemented with a horizontal resolution of 1/16°. These models were validated following the Intergovernmental Panel on Climate Change (IPCC) 20C3M protocol for the period 1950–2000, using observed radiative forcing of Greenhouse gas (GHG) and aerosol that correspond to the 1950s conditions. Afterwards, future climate projections for the 21st century were produced according to the IPCC A1B emission scenario that assumes a balanced emphasis between fossil fuels and other energy sources (Nakićenović et al., 2000). The A1B scenario represents an intermediate case compared both to the more intense A2 and the weaker B1 storyline families, and to the more recent forcing pathways of RCP4.5 and RCP8.5 scenarios.

The consistency of global projections used in this study was evaluated in relation with the more recent scenarios produced in the Fifth Assessment Report (IPCC, 2014). Overall, the performance of the CMIP5 ensemble (IPCC, 2014) is comparable to that of the older CMIP3 ensemble (IPCC, 2007a) (Kharin et al., 2013). Specifically, for the Mediterranean region, the differences are quite little, showing slightly higher values of CMIP5 temperature and precipitations projections compared to CMIP3 (IPCC, 2014). Moreover, in terms of diurnal temperature range, CMIP5 models suggest a higher increase in minimal than in maximal temperatures, which is consistent with CMIP3 (Cattiaux et al., 2013).

Even if CMCC-MED has a quite large horizontal resolution (i.e., around 80–100 km), it is still too low to be used by regional/local impact models. Accordingly, the outputs from these global models were used to implement a regional climate model (COSMO-CLM, Rockel et al., 2008) with an increased spatial resolution, more suitable for climate change studies over all the Esino River basin. Moreover, the high horizontal resolution of COSMO-CLM allows a better description of orography, and thus, an improved representation of small-scale physical processes related to terrain height and land–sea contrast (Bucchignani and Gualdi, 2011). The model has been implemented on the domain 2–20°E, 40–52°N, with a horizontal resolution of about 8 km.

Climatic variables (i.e., temperature, precipitation and evapotranspiration) projections by these models were used to perform river basin catchments hydrological simulations for precipitation and runoff processes using the hydrological model HEC-HMS and the hydraulics model HEC-RAS, both public domain software developed by the United States Army Corp of Engineers. These models were run and calibrated for the current scenario represented by the period 2003–2009, for which observed data were available.

The Hydrological Modelling System (HEC-HMS) simulates the precipitation-runoff processes of dendritic watershed system. It is applied for problem solving in the field of large river basin water supply and flood hydrology and small urban or natural watershed runoff. In the SALT project, the HEC-HMS model was linked with ArcView GIS software using the Geo-HMS extension in order to model the entire Esino River catchment and calculate the main physical parameters (i.e., length and slope of the river course, and drainage path length of the sub-basins) over the entire Esino watercourse, including an estimate of the flows hydrographs used as input by HEC-RAS.

The River Analysis Systems (HEC-RAS) is used to analyze natural and artificial river networks and calculate the free surface profile based on the one-dimensional analysis of both steady and unsteady flows. In addition to the river analysis components, the system contains several hydraulic design features that can be invoked once the basic water surface profiles are computed in order to clearly identify dynamic water surface levels from HEC-RAS simulation, which are allocated to correspondent elements in the groundwater model (FEFLOW), to simulate transmission between the river and aquifer. Results obtained by HEC-HMS for the section of Moie (i.e. the point of the river corresponding to beginning of the case study area) represented the main input useful to simulate the hydraulic levels in the same section with HEC-RAS. The produced outputs were finally used to estimate surface water levels and produce a temporal series of the flows filtering from the river bed to groundwater.

For the future scenarios, a simplified approach was applied to estimate the aquifer recharge based on the assumption that the water infiltration from the river to the groundwater is the main contribution to the groundwater recharge process. Specifically, the process of transmission between the river and the aquifer simulated in the current scenario was projected for the future by applying the same monthly variation of precipitation provided by the climatic models.

Finally, the FEFLOW software, a 3D finite element subsurface model, was applied only to the lower Esino River valley, representing the final case study area for the application of the RRA methodology, in order to simulate flows and transport, and salt intrusion based on density dependent flows. The FEFLOW model provides best-in-class capabilities for porous-media simulations on scales ranging from millimeters to hundreds of kilometers, from milliseconds to thousands of years. The supported processes are: fluid flow, density dependent flow, reactive solute transport, heat transport, saturated and variably saturated and unsaturated conditions, and fracture flow. Within the SALT project, a digital terrain model (DTM) of the Esino coastal aquifer was constructed using stratigraphy data from regional wells, in order to reflect the lower Esino River valley topography and identify and report its four geological units (i.e., gravel–clay, clay–sand, gravel–sand, and the impermeable aquiclude) in the FEFLOW 3D model. Saltwater intrusion into the aquifer was simulated after proper calibration, using data from existing literature regarding recharge processes and Esino River-aquifer exchange.

3.2. Regional Risk Assessment methodology

The spatially resolved Regional Risk Assessment (RRA) methodology applied to the Esino coastal aquifer considers multiple sources of hazards (i.e., changes in the precipitation regime, river flow discharge, and groundwater depth and quality) that can affect the status and conditions of coastal groundwater-dependent natural and human systems (e.g., wells, river, agricultural areas, lakes, and forests and semi-natural environments). The considered impacts are: 1) Groundwater Level Variation (GLV) due to changes in the water table related to the alteration of recharge processes from climate change and excessive pumping of groundwater; 2) Saltwater Intrusion (SI), which refers to the subsurface movement of seawater into coastal aquifer, either from climate variations and consequent fluctuating sea levels or lowering of local wells potentiometric surface due to excessive pumping of groundwater.

Operatively, the RRA methodology can be implemented following six major steps:

1. Definition of the regional risk matrix
2. Hazard assessment
3. Exposure assessment
4. Susceptibility assessment
5. Risk assessment
6. Damage assessment

3.2.1. Definition of the regional risk matrix

The regional risk matrix identifies all the components contributing to the computation of risk in the case study area (i.e., stressors, receptors and impacts) and their relationships (Torresan et al., 2012). It is composed of two distinct sub-matrixes: the vulnerability matrix and the hazard matrix.

The vulnerability matrix (Table 1A) highlights the receptors/targets of analysis, representing relevant components of the case study area that could be affected by climate change impacts, such as GLV and SI. Receptors were selected considering the preferences of a group of stakeholders involved in the SALT project (i.e., public administrations such as coastal municipalities, the province of Ancona, the Marche region) and the availability of spatial territorial data (Table S1). The matrix also includes a range of vulnerability factors, categorized into susceptibility, value and pathway factors, which are clearly defined in Table S2. According to Torresan et al. (2012)), susceptibility factors depict the degree to which targets/receptors could be affected either adversely or beneficially by climate-related hazards and are represented by the ecological and hydrogeological features of the considered region. Value factors represent relevant environmental and socio-economic properties or features of the examined targets or receptors that need to be preserved. Finally, pathway factors denote the physical characteristics of targets/receptors that can influence their possible contact with climate change hazards and thus support the identification of potentially exposed areas.

The hazard matrix (Table 1B) identifies relevant stressors with reference to GLV and SI impacts and the related hazard metrics selected as relevant output from the model chain (Section 3.1).

As described in the next paragraphs, vulnerability factors and hazard metrics will be employed in different stages of the RRA process, from hazard to damage assessment.

3.2.2. Hazard assessment

The hazard assessment is aimed at the spatial characterization of climate change hazard scenarios, which describes potential climatic hazard conditions against which the identified receptors need to adapt in order to maintain their ecological and socio-economical functions. It

Table 1
The regional risk matrix defined for the lower Esino River valley: the vulnerability matrix a) and the hazard matrix b).

A

Receptors	River	Lakes	Agricultural areas	Wells	Forests and semi-natural environments
Impacts on water quality					
Saltwater intrusion	Present depth to saline interface Water salinity	Present depth to saline interface Basin level or extension.	Present depth to saline interface Crop economic value	Present depth to saline interface Wells use typology (drinking, domestic, and irrigation, industrial)	
	River flow (average)	Protection level (e.g. WFD protected areas)			
	River bed slope Protection level (e.g. WFD protected areas)				
Impacts on water quantity					
Groundwater level variations	Present depth to groundwater River flow	Present depth to groundwater Basin level or extension	Present depth to groundwater Crop typology (water requirements) Crop economic value	Present depth to groundwater Average flow/volume pumped	Present depth to groundwater Extension of forests
	Protection level (e.g. WFD protected areas)	Protection level (e.g. WFD protected areas)		Wells use typology (drinking, domestic, irrigation, industrial)	Vegetation cover typology (water requirements)
					Extension of forests Vegetation cover typology Protection level (e.g. WFD protected areas)
Legend	Pathway factors	Susceptibility factors	Value factors		

B

Impacts	Hazard metric
Impacts on water quality Saltwater intrusion	Depth of the saltwater interface
Impacts on water quantity Groundwater level variations	Groundwater mean level

is based on the aggregation of multiple hazard metrics/variables defined within the hazard matrix.

The assessment was focused on seasons (i.e., winter, spring, autumn and summer) to determine how changes in the precipitation regime of the reference timeframe 1971–2000 could be influenced by projected climatic trends for the future timeframe (2071–2100) at seasonal level. The calibration was made using data available for the case study area from the year 2000 to the year 2008. Even if this interval is relatively short, it can be considered as representative for the region under investigation because it include extreme years with regard to the quantity of precipitations and to the temperatures (e.g. the year 2003 was an extremely dry and hot year, while 2007 was an extremely wet and cold year). The analysis was performed considering seasonal precipitation patterns referred to three different representative years in the present and future timeframe (i.e., the driest, the average and the wettest years), in order to provide a complete description of the investigated effects. In this application, different precipitation scenarios (s) were defined to represent the future seasonal average of the precipitation regime with reference to the four different seasons and the three representative years, and they were considered as the future climate change scenarios useful to assess climate-related hazards for each examined impact (k). Generally models estimated a little increase of precipitations in winter (less than 10%) and a decrease in the other seasons (between 10% in spring and 20% in summer). Climatic information was used to estimate the recharge of the aquifer by applying the percentage of future monthly variation of precipitation to the temporal series of monthly infiltration into the groundwater estimated for the current scenario in around 5.3 L/(s km^2), coherently with literature data (Bassi, 1972). This value, multiplied by the surface of the aquifer, allowed to estimate the annual volume of water infiltration, i.e., around 23 mm^3/year. The consequence of the precipitations' reduction in future climate brings to a decreased value of aquifer recharge of about 21 mm^3. In order to evaluate extreme events, simulations were produced also increasing the quantity of water extracted from wells, but results showed that even if the situation will be worse than an average year, the level will not dramatically decrease due to the increase of the mean sea level, and even if saltwater will move more inland, will not step into for more than few hundred meters from the coastline, as will be described also in the results (Section 4.1).

For the GLV impact, the hazard is represented by the increase of future water table depth, as a result of climate changes and anthropogenic activities. This is specifically identified by the difference between the future groundwater depth and the present groundwater depth, where a reduction in water table is expected. The GLV hazard is based on daily mean groundwater depths for the case study area that were averaged to estimate the seasonal mean groundwater depth.

For SI impact, the hazard is related to the potential intrusion of saltwater into the Esino aquifer due to the reduction in the water table as a consequence of significant pressures from human activities, climate changes and concomitant sea-level rise. According to the CMCC-MED model, the sea level of the Adriatic Sea at the end of the 21st Century might be about 22 cm higher than the mean sea level found for the

reference period (1961–1990) as a consequence of the changes in the water density (steric effect). This value could increase due also to the ice melting of a value ranging between 18 and 59 cm. In order to include both the components, the sea level-level rise value was finally estimated in 60 cm, considering 22 cm of increase due to steric component and 38 cm (average value of the range) due to the ice melting.

The SI related hazard is thus identified by changes in the saline interface depth (saline wedge) between freshwater in the Esino aquifer and the Adriatic seawater, taking into account the potential consequences of SLR. Such changes were derived considering the difference between saline wedge depth values in the reference period and in the future timeframe (2071–2100). The saline interface was identified based on the Italian standards for groundwater quality (DPR 236/1988; DPR, 1988), i.e., where the concentration of saltwater in the Esino aquifer due to the Esino River-aquifer exchange and given by the model is higher than the threshold of 1300 mg/L.

In more detail, potential changes in the saline interface depth were analyzed with reference to each season, i.e., considering the seasonal average values of the saline interface depth in order to characterize potential SI hazard at seasonal scale.

3.2.3. Exposure assessment

Exposure assessment is aimed at identifying and classifying possible impacted areas or valuable receptors. It aggregates the estimated hazard metrics ($h_{s,k}$) with the identified pathway factors (p), according to relevant exposure functions defined for each of the investigated climate change impacts.

Exposure analysis for GLV and SI impacts (Table 2) resulted in exposure scores in the range between a minimum value of 0 and a maximum value of 1. The minimum value refers to no exposure of the areas/receptors, while maximum value represents extreme exposure of areas/receptors compared with other receptors in the case study area. Accordingly, exposure scores do not allow to estimate climate change exposure in absolute terms, rather they provide a relative evaluation of potential areas or receptors exposed to climate-related hazards.

Such equations were based on the following specific assumptions: 1) the more variations in groundwater/saline interface depth, the more receptors lying on top are harmed; 2) the pathway through which groundwater/saltwater can reach receptors was defined as the groundwater/saline interface mean depth, which in practice represents the soil lying between the ground surface and water table/saline interface; 3) the increase/decrease of groundwater/saline interface depth is impacting only receptors lying at a distance equal or less than a predefined susceptibility threshold (s_1 or s_2). The values s_1 and s_2 depict changes in groundwater/saline interface depth that could impact specific receptors lying at a distance equal or less than a predefined value. They were selected based on available literature's data and on the judgements of different experts/researchers, and relevant stakeholders who participated in the various SALT project workshops. The values of s_1 and s_2 were defined as 3 m for all the receptors in the entire considered region, except in a buffer zone of 50 m around the river mouth where were 2 m.

Table 2
Exposure equation for the GLV and SI impacts.

	Equation	Legend
Impacts on water quality Eq. (1): groundwater level variations	$E_{glv,s} \begin{cases} 0 & pf_1 > s_1 \\ \min(\frac{pf_1 + h_{glv,s}}{s_1}, 1) & \text{otherwise} \end{cases}$	$h_{glv,s}$ = Amount of positive difference between forecasted depth of groundwater in scenario s and present depth (positive number). pf_1 = Distance of groundwater from the ground level at present (positive number). s_1 = Distance of groundwater from the ground level which imply an effect of groundwater level decrease on receptors.
Impacts on water quantity Eq. (2): saltwater intrusion	$E_{si,s} \begin{cases} 0 & h_{si,s} = 0 \\ \max(1 - \frac{pf_2 - h_{si,s}}{s_2}, 0) & \text{otherwise} \end{cases}$	$h_{si,s}$ = Amount of positive difference between present depth of saltwater and forecasted depth in scenario s (positive number). pf_2 = Present depth of saltwater from the ground level (positive number). s_2 = Distance of saltwater from the ground level which imply an effect of saltwater level increase on receptors.

A different technical threshold (i.e., 10 m) was also chosen for all the considered shallow wells, considering the localization of the well filters. These thresholds allow analysts to identify areas and receptors, which are connected to the shallow groundwater aquifer at present and to exclude areas not directly linked to such aquifers.

The exposure analysis for the GLV impact was focused on potentially exposed groundwater-dependent natural and human systems (i.e., agricultural areas, river, lakes, forests and semi-natural environments). A higher increase in groundwater depth corresponds to an increase of the potential harm for the considered receptors.

As far as the SI impact is concerned, the exposure analysis was focused on the potential exposure of the same receptors to future changes in saline interface depth, due to the potential movement of saline wedge interface inland. A higher potential harm for the considered receptor is caused by a decrease of the saline interface depth.

3.2.4. Susceptibility assessment

The susceptibility assessment was carried out using the susceptibility factors identified in the vulnerability matrix (Table 1A). These factors have been classified assigning susceptibility scores according to data from existing literature and expert judgements. Thus, susceptibility classes were determined by thresholds that reflect variations in the degree to which the case study area may be affected by climate-related impacts. In accordance with specific features, for each factor a discrete set of classes and related scores were defined and evaluated, as reported in Table S4. The susceptibility scores represent the relative susceptibility value of each single class, ranging from 0 (i.e., no susceptibility) to 1 (i.e., maximum susceptibility).

As far as the GLV impact is concerned, *vegetation cover typology* and *crop typology* factors were defined according to the Corine Land Cover 2006 map, aggregating according crops typologies with similar water needs. The highest score (i.e., 1) was assigned to the most water demanding crops, and intermediate and low scores (i.e., 0.7 and 0.3) were assigned to others. For the *extension of forest* and *basin extension* factors, classes were defined by dividing factors' extension (km^2) range in 5 and 2 classes, respectively, according to the equal interval method (ESRI Inc., 1995), in order to normalize them in the range of 0–1. Thus, susceptibility scores were assigned considering that the smaller is the receptors' surface area, the higher their susceptibility to hazards related to groundwater depth decrease. In addition, for *river flow* and *average volume yearly extracted from wells* factors, classes were defined using a similar approach, but considering relevant measured data provided by partners involved in the SALT project (Table S3). For such factors, susceptibility scores were assigned in the range from 0.2 (i.e., lowest susceptibility) to 1 (i.e., highest susceptibility). This is because the more the average volume of water yearly is extracted from wells, the more these wells will be sensitive to GLV related hazard.

With regard to the SI impact, for the *basin extension* factor, classes were defined in consideration of the two lakes' extension (km^2), and scores were assigned according to the same procedures adopted for GLV impact and explained above. The *water salinity* factor, which is related to the Esino River aquifer subsurface flow modeling data obtained from four different gauge stations, five classes were defined using the equal interval method (ESRI Inc., 1995), and susceptibility scores assigned based on the following assumption: higher conductivity would result in higher susceptibility to saline contamination in unconfined coastal aquifer. In addition, classes related to *river flow* and *river bed slope* factors were defined using the aforementioned equal interval method, considering data related to the Esino River flow (m^3/s) and its hydro-morphology respectively. The related susceptibility scores were assigned according to the following assumption: higher river flows in terms of the average will lead to lower susceptibility of coastal aquifer freshwater to saline contamination, since higher river flows move more water toward the seabed and thus, increase the dilution of saltwater.

According to the vulnerability matrix in Table 1A, susceptibility factors were not identified for wells and agricultural areas. However, a maximum susceptibility score (i.e., 1) was assigned to wells with reference to SI impact because it was assumed that salt water could compromise their use. Agricultural areas were conservatively assigned a susceptibility score equal to 1 because available data did not provide enough detailed information about vegetation cover typology, impeding to distinguish the different susceptibility of plants (e.g., halophytes and glycophytes) to saltwater.

The same weight of 1 was assigned also to all the considered factors in order to give the same importance to all susceptibility parameters in the computation of susceptibility. Finally, susceptibility scores were aggregated using the MCDA function "Probabilistic or", as shown in Eq. (3), to provide the relative rank of areas and receptors more sensitive to GLV and SI impacts.

$$S_k = \otimes_i^n \left[sf'_{i,k} \right] \tag{3}$$

where:

S_k Susceptibility score of the cell to the impact k;
$\otimes$ "Probabilistic or" function;
$sf_{i,k}'$ Normalized ith susceptibility factors related to the impact k;

Using the "Probabilistic or" function, the result of the susceptibility assessment S_k is the maximum (i.e., 1) if just a susceptibility factor $sf_{i,k}'$ assumes the maximum value (i.e., 1). Moreover, all susceptibility factors $sf_{i,k}'$ contribute in the increase of the final susceptibility score. Accordingly, the higher is the number of susceptibility factors $sf_{i,k}'$, the higher is the final susceptibility score S_k.

3.2.5. Risk assessment

The risk assessment is aimed at identifying and ranking areas and receptors at risk to GLV and SI impacts in the lower Esino river valley. However, within the RRA methodology, regional risks estimations are not absolute predictions of risks related to climate change; rather they provide relative classifications about areas and targets that are likely to be affected by climate change impacts more severely than others in the same region. In this context, risk assessment is based on relative risk scores ($R_{k,s,i}$) obtained for the investigated impacts as the product of exposure scores $E_{k,s}$ (Section 3.2.3) and the susceptibility scores $S_{k,i}$ (Section 3.2.4) according to the risk function expressed by Eq. (4).

$$R_{k,s,i} = E_{k,s} \cdot S_{k,i}. \tag{4}$$

where:

$R_{k,s,i}$ Relative risk related to hazard k, scenario s and receptor i;
$E_{k,s}$ Exposure related to hazard k, in the scenario s;
$S_{k,i}$ Susceptibility related to hazard k, and receptor i.

The estimated relative risk scores vary from 0 to 1, in which 0 means no risk (i.e., there is no exposure or no sensitivity to the considered impacts) and 1 means higher risk for considered receptors/areas in the region.

3.2.6. Damage assessment

The damage assessment provides the relative estimation of potential social, economic and environmental losses of receptors and areas at risk in the considered region. It considers the integration of risk scores (Section 3.2.5) with value scores; the latter is obtained from the estimation of environmental and socio-economic features of receptors and aggregated using a specific value function (i.e., additive procedure). The estimation of receptors' value scores requires the definition of classes and associated scores for the selected value factors. Value factors defined in the damage assessment of GLV and SI impacts (Table S4) include *protection level*, *crop economic value*, *and extension of forest*,

vegetation covers typology and *well uses typology*. These factors were selected considering data from existing literature related to the case study area and opinions from relevant stakeholders.

The value factors classification followed the same procedure of the one proposed in Section 3.2.4 for susceptibility factors. Qualitative value factors are represented by *protection level*, *vegetation cover typology* and *well use typology*. The classification of the *protection level* factor was based on the level of importance of the regulation which defined each protected area: the European level (i.e., SPAs and SACs sites of Natura 2000 network) had the highest value score (i.e., 1), national and regional Parks and Reservoirs had an intermediate score 0.6, while unidentified areas were classified with the lowest score (i.e., 0.2). As far as *vegetation cover typology* is concerned, the value score was assigned based on the economic and naturalistic value of the vegetation cover: forests had the highest score while scrub/herbaceous vegetation and sparse vegetation had an intermediate (i.e., 0.7) and the lowest (i.e., 0.3) value scores respectively. Finally, *well use typology* scores were defined based on the different categories of wells usage (e.g., domestic, industrial, agriculture, irrigation, drinking and other purposes). The most important uses, i.e., domestic/drinking, were assigned 1, while less important uses, i.e., industries supply, were assigned 0.7 and least important use, i.e., agriculture/irrigation, were assigned 0.5.

The classification of the two quantitative factors, i.e., *crop economic value* and *extension of forest*, was made dividing the range of values of each factor into five equal intervals.

Value factors are aggregated using the function reported in Eq. (5) in order to calculate a relative value score representing the environmental and socio-economic value, in non-monetary terms, of the considered receptors.

$$V_j = \frac{\overline{\sum_{i=1}^{n} \left[vf'_{i,j} \right]}}{n} \tag{5}$$

where:

V_j Value scores related to the receptor i;
$vf'_{i,j}$ Normalized jth value factors related to the receptor i;
n Number of value factors.

Finally, the damage function expressed by Eq. (6) is applied to integrate the calculated risk scores (Section 3.2.5) with the aggregated value scores, to determine possible environmental and socio-economic loss, in non-monetary terms, for areas/receptors with respect to GLV and SI impacts in the future scenarios.

$$D_{k,s,i} = R_{k,s,i} \cdot V_i \tag{6}$$

Where:

$D_{k,s,i}$ Damage scores related to hazard k, and a receptor i in scenario s,
$R_{k,s,i}$ Risk scores related to hazard k and receptor i in scenario s,
V_i Value scores of receptor i.

In this way, damage scores were calculated for all the examined receptors in the case study area, including relevant statistics (e.g., percentage of the total surface area of each receptor associated to each damage class and
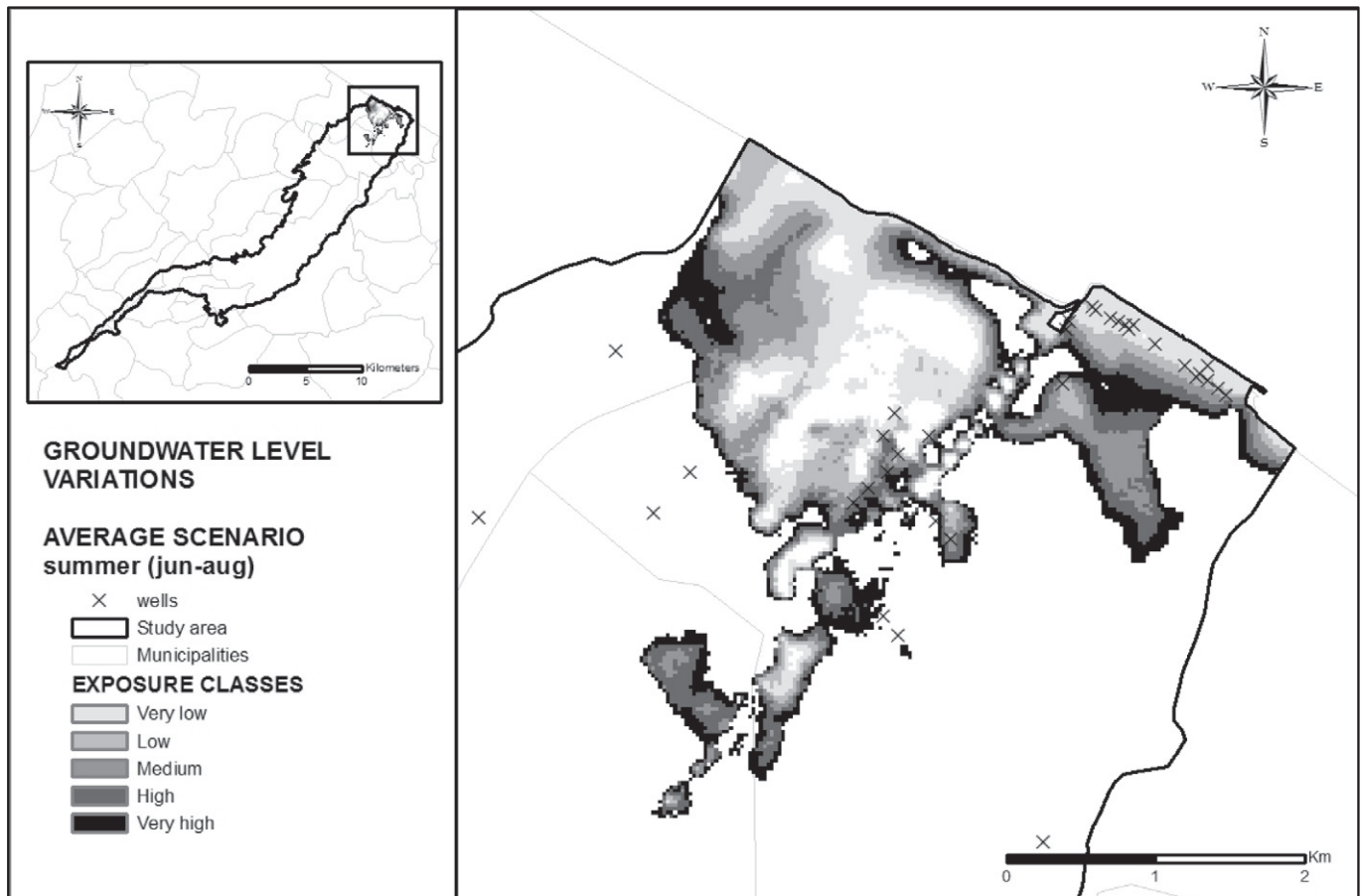

Fig. 4. Exposure map for the Groundwater Level Variation impact, summer season.

territorial surface of each receptor with higher damage scores for each administrative unit, etc.).

4. Results and discussion

The main results of the RRA include GIS-based maps describing spatial changes in exposure, susceptibility, risk and damage to GLV and SI impacts. In addition, relevant statistics were calculated to further analyze these maps, in order to systematically and quantitatively characterize future climate change trends, which could affect areas and receptors in the lower Esino River valley.

In order to apply the RRA methodology, all input data (Table S3) were first georeferenced applying to all the same coordinate system and then converted into raster files (i.e. TIFF format) with a resolution of 25 m, representing the highest feasible spatial detail in relation to the available dataset.

The relevant GIS maps and their related statistics from the case study area application are thus presented and discussed below.

4.1. Exposure maps

Exposure maps for GLV impact revealed slight differences among different seasons, within the same analyzed scenario (Section 3.2.2), and negligible differences comparing different scenarios (i.e., three consecutive dry or wet years or an average year). Thus, based on the assumption that there will be continual variations in the precipitation regimes over consecutive years rather than the presence of three consecutive extremely dry or extremely wet years, the current analysis was focused on the summer season (i.e. the driest one) of an average year. Additionally, a sea-level rise of 60 cm, representing the worst value of rise in the mean sea-level, was used within the selected scenarios.

Climate change scenarios are widely considered as a key tool for risk assessment (Wilby et al., 2009). Particularly, the comparison of different possible and alternative situations (i.e. worst/best case scenarios) can be useful to inform the decision-making process and prioritize responses (UKCIP, 2003). All climate scenarios used in the exposure assessment are affected by a certain degree of uncertainty that is amplified by combining several models through a model chain (Baruffi et al., 2012). Particularly, uncertainty sources relates to assumptions about radiative forcing and emissions scenarios and to the choice of climate, hydrological and hydrogeological models and their parameterization (inter- and intra-model variability). Even if there is not enough information to provide a comprehensive uncertainty analysis (or a probabilistic forecast) of exposure to hazard, the study is based on the evaluation of ranges of potential outcomes, with particular attention to high consequence scenarios (precautionary principle).

The exposure map (Fig. 4) shows that potentially exposed areas are limited to the region closer to the coastline and a few kilometers inland, where the present groundwater depth is low due to the water table lying close to the ground's surface and mean groundwater depth is expected to decline significantly, with likely consequences for superficial dependent systems (e.g., wells, lakes and river etc.). Conversely, unexposed areas are those in which present groundwater depth is already too high to support superficial natural and human systems and those in which mean groundwater depth is not expected to decline or is expected to rise.

Significant statistics were calculated for the considered future scenario focusing on each receptor, as reported in Fig. 5. The table of Fig. 5A shows the total exposed surface (km^2) of each receptor in the five exposure classes and indicate the percentage of exposed surface of each receptor. By the table, it is evident that agricultural areas will have the largest total exposed surface (almost 3.7 km^2) distributed in all the exposure classes, while superficial water bodies, forests and semi-natural environments will have a smaller total exposed surfaces. The percentage of exposed surface, except for lakes, is around or lower than 5% of the total surface of each receptor. Based on these data, the percentage of exposed surface within each exposure class has been depicted in Fig. 5B. According to these statistics, forests and semi-natural environments are projected to
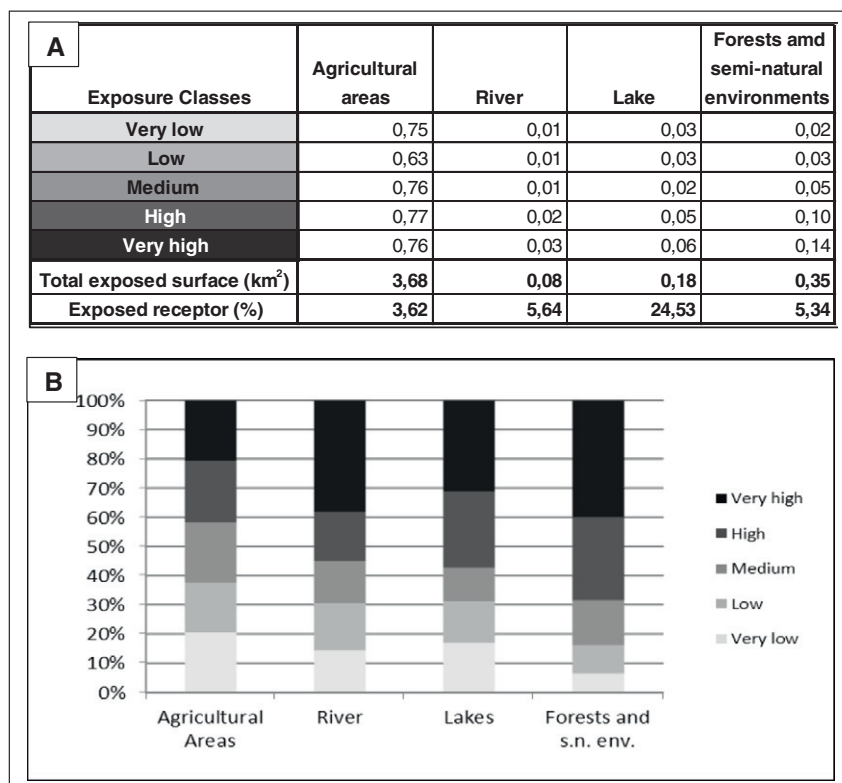
A Exposure Classes	Agricultural areas	River	Lake	Forests amd semi-natural environments
Very low	0,75	0,01	0,03	0,02
Low	0,63	0,01	0,03	0,03
Medium	0,76	0,01	0,02	0,05
High	0,77	0,02	0,05	0,10
Very high	0,76	0,03	0,06	0,14
Total exposed surface (km^2)	3,68	0,08	0,18	0,35
Exposed receptor (%)	3,62	5,64	24,53	5,34

Fig. 5. A) Distribution of the territorial surface (km^2) associated with each exposure class for the Groundwater Level Variation impact, average scenario, summer season. B) Distribution of the percentage of exposed surface associated with each exposure class.

have nearly 70% of their total exposed surface associated to the very high and high exposure classes; superficial water bodies will have approximately 55% of their total exposed surface in the two higher exposure classes, while a little more of the 40% of agricultural areas' total exposed surface is included in the high and very high exposure classes.

Similar statistics were calculated also for shallow wells, and these revealed a small percentage of exposed wells in the future scenario. In particular, less than 3.5% wells will be exposed to the GLV-related hazard.

Exposure maps were produced also for SI impact considering the four different seasons. These maps revealed similar exposure when comparing the same season in different scenarios. In this analysis, SI exposure map for the winter season and average scenario was selected since it shows the highest exposure. Future improvements of the assessment concern a quantitative evaluation of the likelihood or probability of occurrence of the analyzed hazards (e.g., based on multiple observations or model ensemble runs) in order to associate a level of uncertainty (or confidence) to relevant policy findings.

Fig. 6 presents the exposure map for the considered region showing potential limited exposure to the SI related hazard within the coastline (i.e., changes in saline interface depth will only be restricted to the coastal strip). Consequently, SI related impact might not bring serious threats to the considered receptors, which are not directly dependent on coastal groundwater aquifers, except few over utilized wells located along the coastline. For this reason, there are neither detailed analyses of exposure related to SI nor specific statistics calculated for the examined receptors. However, such outcomes agree with previous analyses (e.g., Alberti et al., 2009), regarding saltwater intrusion impacts in this region, which had foreseen significant annual variations in saltwater intrusion based on future climate change scenarios only at the coastal

strip. Further, also some recent studies confirmed that the increase of the mean sea-level is not always representing a threat to coastal aquifer, which can experience more sever impacts due to the increment of the extraction for anthropic uses (Ferguson and Gleeson, 2012; Taylor et al., 2012).

4.2. Susceptibility map

The susceptibility map in Fig. 7 represents the sensitivity of receptors to GLV related impacts. According to this map, almost all agricultural areas, forests and semi-natural environments are classified with high and very high susceptibility scores, due to the prevalence, in the considered region, of permanent crops and annual/pasture/arable crops, which are characterized by high or very high susceptibility scores according to their water requirement. With regard to the susceptibility scores of forests and semi-natural environments, the final score is mainly due to the extension of forests, which are quite wide with a low level of fragmentation, while the vegetation cover typology, has a lower influence on the final susceptibility assessment.

Finally, the susceptibility scores for the superficial water bodies (e.g., Esino River and lakes) are quite heterogeneous, ranging from low to medium classes. The spatial distribution does not show the presence of hot spots or cold spots (i.e., areas characterized by high or low susceptibility scores). The medium and high susceptibility scores assigned to wells is mainly due to the average volume of water extracted per year, and are distributed all over the considered region.

As far as the susceptibility to SI impact is concerned, Figure S1 highlights that superficial water bodies located within the coastline, such as lakes and the Esino River, are characterized by medium to high susceptibility scores. This is due to the low average flow rate of the Esino River
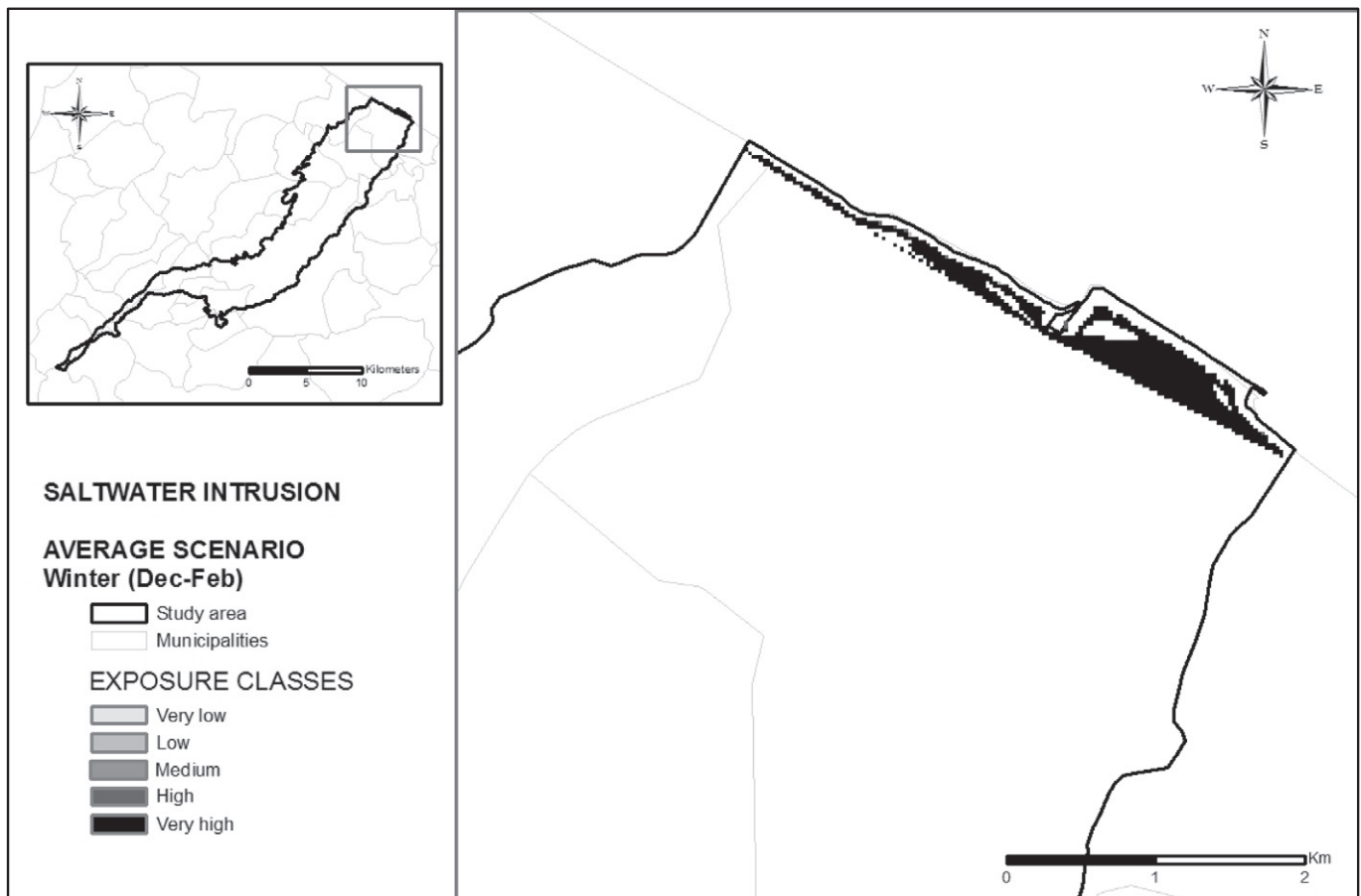

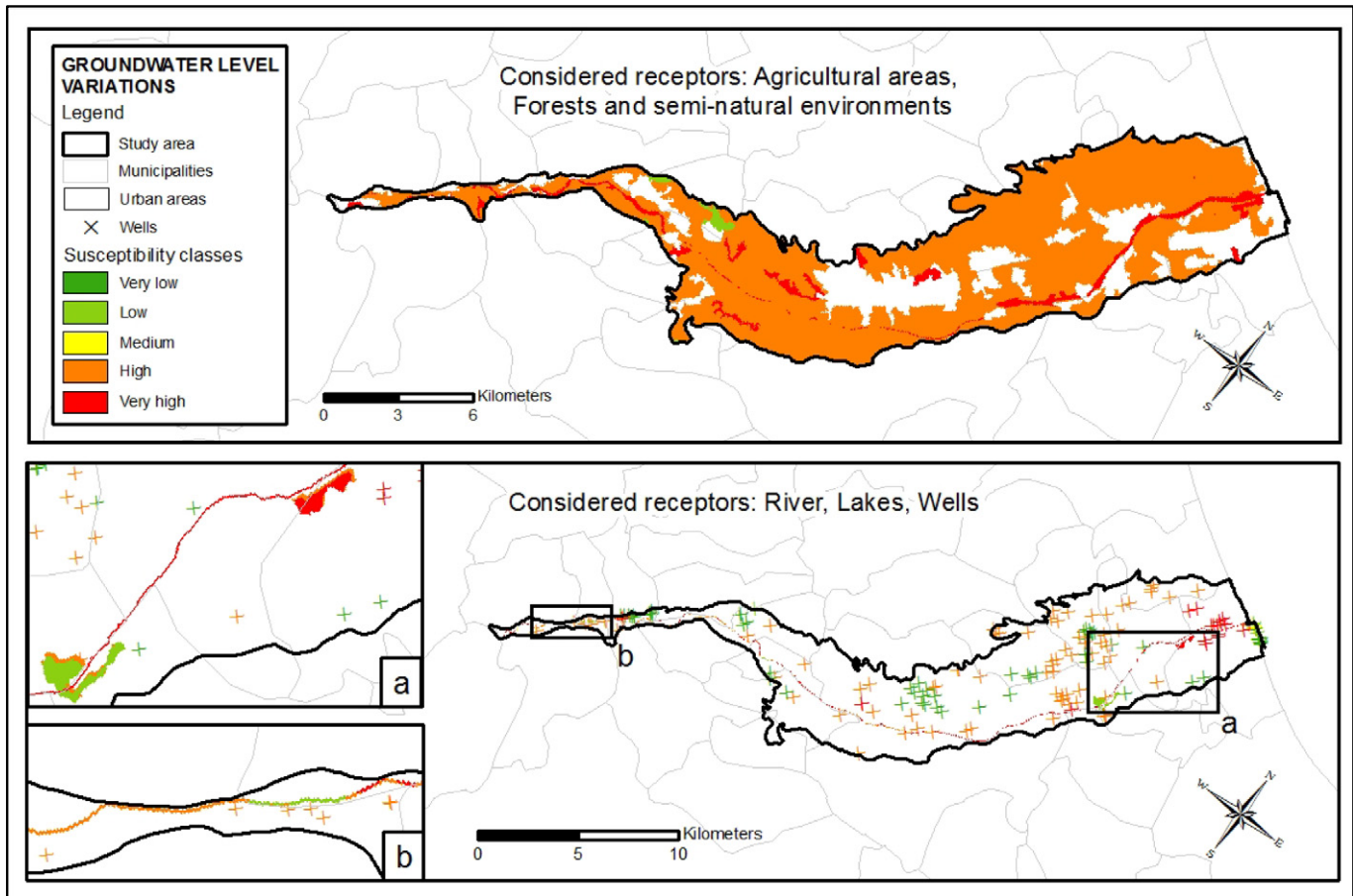**Fig. 6.** Exposure map for the Saltwater Intrusion impact, winter season.

Fig. 7. Susceptibility map for the Groundwater Level Variation impact.

that would result in high susceptibility to saline contamination. Finally, according to the defined methodology (Section 3.2.4), agricultural areas and wells are characterized by the maximum susceptibility score (i.e., 1).

These results suggest that some measures could be defined in order to reduce the susceptibility of the region. In particular it could be recommended to adopt crops with a lower water demand and preferably do not requiring artificial irrigation in the summer period. A reduced request of water for agriculture, coupled with the adoption of good management actions (e.g. use recycled wastewater for industrial purposes) can contribute to keep low the volume of water extracted from wells.

Susceptibility is probably the most difficult factor to represent quantitatively in the risk assessment. In fact, very few data exist on the degree of damage of various elements at risk from different types of hazards (Crozier and Glade, 2005). Moreover, susceptibility is characterized by inherent levels of uncertainties (e.g. subjectivity of experts' judgements, difficulty of considering dynamic vulnerabilities) that are partially addressed providing a traceable account of assumptions and steps used in the process. A more accurate evaluation of susceptibility should encompass a sensitivity analysis applied to the ranking process (i.e. selection of scores and weights) and the application of group decision theory to find a consensus among different experts' judgements. Finally, projections related to the susceptibility factors could be used to model future spatial patterns of vulnerable targets and attributes, to be combined with future exposure scenarios in the final estimate of risks.

4.3. Risk map

Risk maps for the GLV impact for the considered receptors and areas, coherently with the exposure maps, have been focused on the summer

season, according to the observation in Section 4.1 and with the aim to analyze the extreme effects of a dry climate in the future scenarios.

The risk map presented in Fig. 8 shows that areas at risk are concentrated only close to the Esino River mouth in a coastal strip of a few kilometers. Moreover, it emerges that agricultural areas are classified mainly in the three lower relative risk classes (i.e., from very low to medium). This is due to the exposure score, as the classification of susceptibility in that area was quite homogeneous. The other three receptors show a more homogeneous spatial distribution among the five relative risk classes.

Several statistics have been calculated related also to the relative risk assessment (Fig. 9). Looking at the total surface potentially at risk (km^2) of the considered receptors in each relative risk class (Fig. 9A) and the related graph with the percentage of surface potentially at risk (Fig. 9B), it is evident that agricultural areas are the less threatened receptor, with less than 4% of surface at risk, more than 80% of surface at risk classified within the three lower classes (i.e., from very low to medium) and less than 5% in the very high relative risk class. The other three receptors have a greater percentage of area at risk, though around 50% of their surfaces at risk belong to the three lower classes, while the surface percentage in the high and very high classes is quite different for each receptor. Lakes and forests and semi-natural environments have around 20% of their surfaces at risk in the very high risk class, while the same class for Esino River covers about 40% of its surface at risk.

To summarize, the analyzed relative risk map and the related statistics show that GLV related impacts in the summer season would bring limited effects on the case study area, especially on agricultural areas.

Regarding shallow wells' risk assessment related to GLV impact, risk maps and related statistics for the future scenarios and seasons were not produced, considering the very small percentage of exposed wells in the
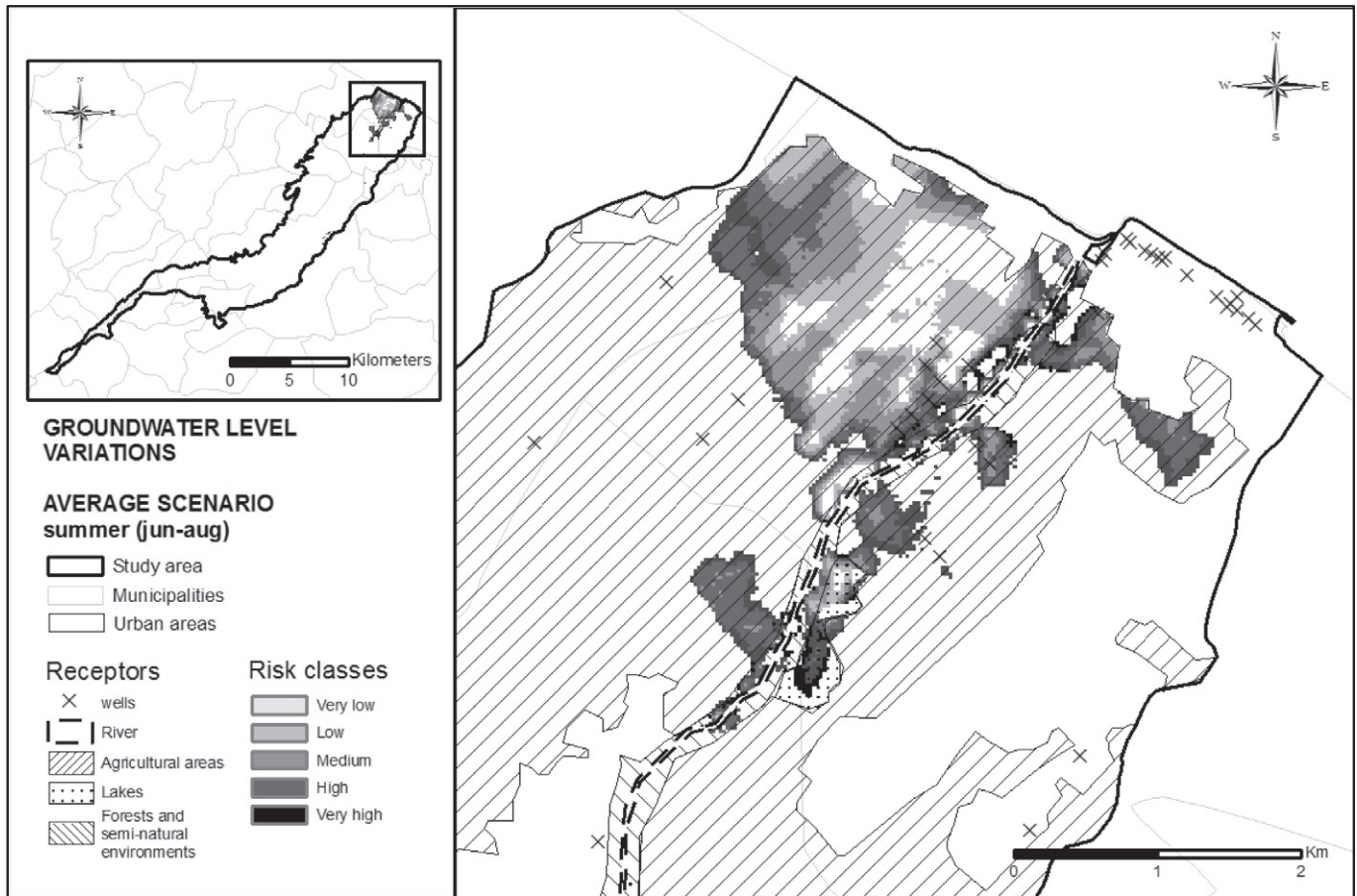
Fig. 8. Risk map for the Groundwater Level Variation impact, summer season.

case study area. Similarly, SI impact risk analysis for the examined scenarios and seasons were not considered, due to the limited exposure of receptors to seawater intrusion within the coastal strip. The limited risk suggests that local authorities should continue managing carefully the water resource, but if the consumption of water will not suddenly increase, no particular measures will be required to adapt to climate change.

4.4. Damage map

The last output is represented by damage maps that have been produced integrating risk and value maps, as described in Section 3.2.6. Value maps related to the GLV impact are reported in Fig. S2. Agricultural areas show values which range from very low, close to the coastline, to very high, in the part of case study area far from the coastline due to the presence of high value crop productions. The other receptors, instead, have usually more homogeneous value scores and are mainly classified in the lower value classes.

Seasonal damage maps were successively produced, and Fig. 10 depicts the damage map for the summer season of the average scenario. The map shows very limited or no damages for all the considered receptors, including areas close to the Esino River and lakes, which are projected to experience higher surface percentages in the very high risks class in the future scenario (i.e., summer season of the average year), as previously highlighted in Section 4.3.

Overall, the damage analysis shows that changes in coastal groundwater levels due to the future predicted variations in the precipitation regimes and water table depth at seasonal scale, will likely have few consequences on surface water bodies (Lakes and Esino River) and on a large part of the natural systems and agricultural areas; because

such most valuable receptors – according to value maps – are located where very low or null exposure is predicted.

Finally, SI impact damage analysis for the examined scenarios and seasons were not considered, due to the limited exposure of receptors to seawater intrusion within the coastal strip.

Coherently with the risk maps, the results of the assessment confirm that the region is well managing water resources, thus future climate change should not pose particular threat to the region. By the way is advisable to keep the situation under control, improving management practices and limiting the water consumption in agriculture and for industries. A more detailed cost benefit analysis could support the definition of the best suite of measures useful to maintain a sustainable use of groundwater resources in the analyzed region.

5. Conclusions

The main objective of this paper was to illustrate a risk-based methodology for the assessment of climate change impacts on coastal aquifers, based on an integrated modeling chain that includes: 1. global and regional climate models, providing climate change projections and relative hazards at case study level; 2. local hydrological and hydrodynamic models, which translate the climate signal into impacts on groundwater resources.

The obtained results highlight how climate change could pose minor negative effects with different magnitudes and severity on the Esino river basin. The observed effects are impacts related to variations in groundwater levels and, to a least extent, impacts related to changes in the saltwater interface depth. In particular, results point out that seasonal variation in climate changes will slightly affect availability of surface waters.
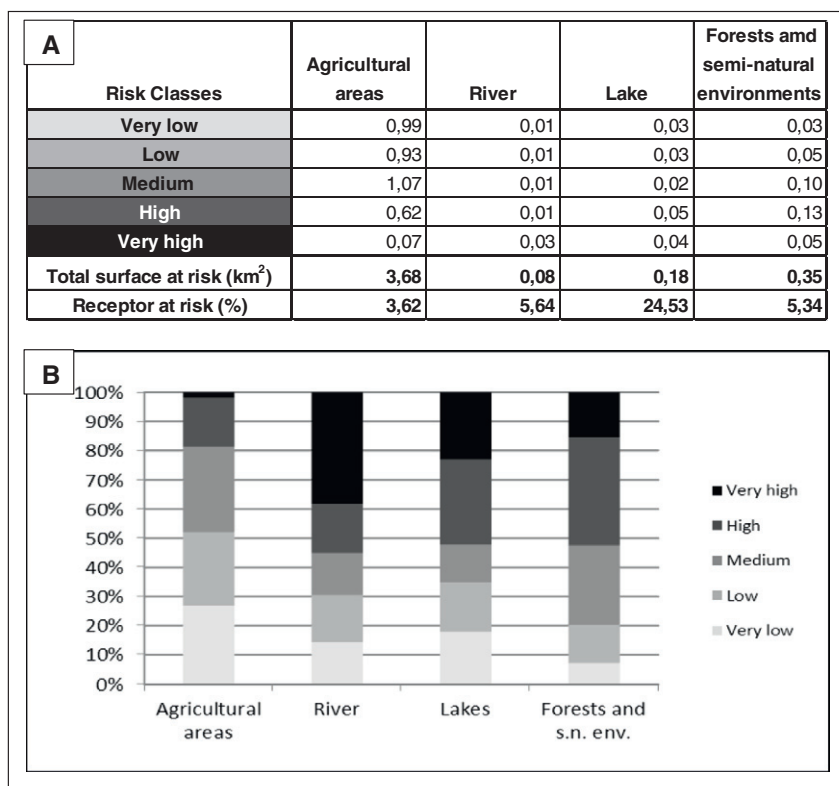
Risk Classes	Agricultural areas	River	Lake	Forests amd semi-natural environments
Very low	0,99	0,01	0,03	0,03
Low	0,93	0,01	0,03	0,05
Medium	1,07	0,01	0,02	0,10
High	0,62	0,01	0,05	0,13
Very high	0,07	0,03	0,04	0,05
Total surface at risk (km^2)	3,68	0,08	0,18	0,35
Receptor at risk (%)	3,62	5,64	24,53	5,34

Fig. 9. A) Distribution of the territorial surface (km^2) associated with each relative risk class for the Groundwater Level Variation impact, average scenario, summer season. B) Distribution of the percentage of surface at risk associated with each relative risk class.

The proposed methodological approach is flexible and adaptable in terms of spatial and temporal scales. In fact, RRA can be applied to other coastal aquifers in Italy or in other countries, customizing hazard projections, susceptibility and value factors according to the specific characteristics of the case study. Saltwater intrusion and other ground-water related impacts due to climate change and anthropogenic activities (e.g. overexploitation of the aquifer for agriculture or industry) are evident in other Italian regions such as Emilia Romagna, (Antonellini et al., 2006; Giambastiani et al., 2007), Tuscany (Grassi and Netti, 2000) or Puglia (Cotecchia et al., 2005) and in many other countries. All these areas could represent interesting cases for the application of the proposed approach.

One of the main criticalities of the described application is represented by the level of uncertainty of the hazard assessment. In fact all the models are characterized by different levels of uncertainty over space and time that are even amplified in the modeling chain. Moreover, further research
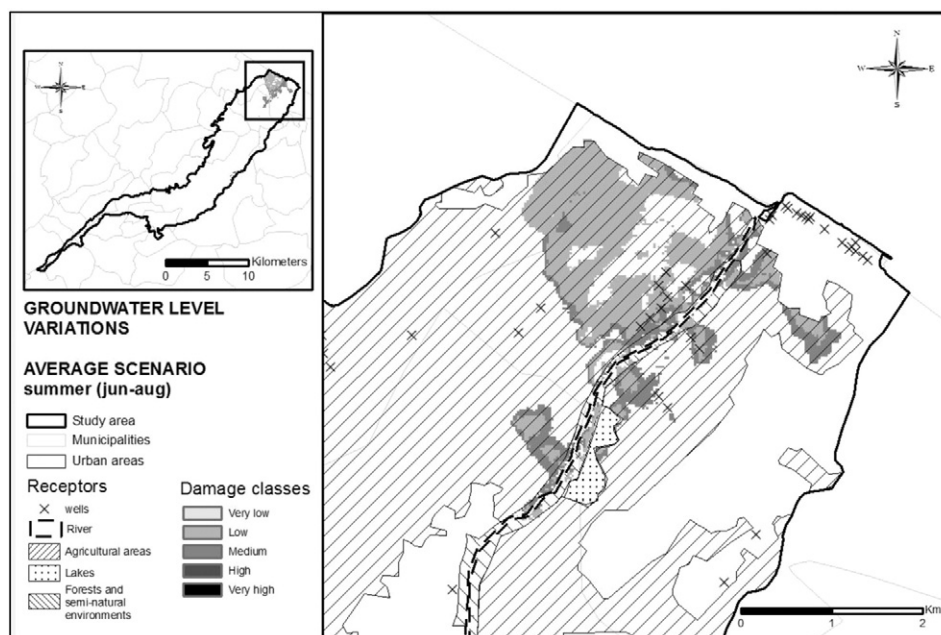

Fig. 10. Damage map for the Groundwater Level Variation impact, summer season.

development is foreseeable by using additional datasets and monitoring data to improve the assessment of the spatial vulnerability of targets and areas to multiple stressors within the considered region.

Acknowledgments

Appendix A. Supplementary data

Supplementary data to this article can be found online at http://dx.doi.org/10.1016/j.scitotenv.2015.06.111.

References

Abd-Elhamid, H.F., 2010. A simulation–optimization model to study the control of seawater intrusion in coastal aquifers (PhD dissertation) University of Exeter, England.
Abd-Elhamid, H.F., Javadi, A.A., 2011. A cost-effective method to control seawater intrusion in coastal aquifers. Water Resour. Manag. 1–26.
Alberti, L., Francani, V., La Licata, I., 2009. Characterization of salt–water intrusion in the lower Esino Valley, Italy using a three-dimensional numerical model. Hydrogeol. J. 17 (7), 1791–1804.
Antonellini, M., Mollema, P., Giambastiani, B., Banzola, E., Bishop, K., Caruso, L., La Penna, E., Mischio, A., Pellegrini, L., Rizzo, E., Sabia, M., Ulazzi, E., Gabbianelli, G., 2006. Saltwater intrusion in the coastal aquifer of the southern Po plain. What future is there for our coastal freshwater? ADRIA 2006 International Geological Congress on the Adriatic area, Urbino (IT) 19–20 June 2006, pp. 23–24.
Baba, A., Tayfur, G., Gunduz, O., Howard, K.W.F., Friedel, M.J., Chambel, A., 2011. Climate change and its effects on water resources: issues of national and global security. Springer, p. 3.
Barron, O.D., Pollock, R., Crosbie, W., Dawes, S., Charles, F., Mpelasoka, S., Aryal, M., Donn, M., Wurcker, B., 2010. The impact of climate change on groundwater resources: the climate sensitivity of groundwater recharge in Australia. Water for a Healthy Country Report.
Barron, O., Silberstein, R., Ali, R., Donohue, R., McFarlane, D.J., Davies, P., Hodgson, G., Smart, N., Donn, M., 2012. Climate change effects on water-dependent ecosystems in South-western Australia. J. Hydrol. 475, 434–435.
Baruffi, F., Cisotto, A., Cimolino, A., Ferri, M., Monego, M., Norbiato, D., Cappelletto, M., Bisaglia, M., Pretner, A., Galli, A., Scarinci, A., Marsala, V., Panelli, C., Gualdi, S., Bucchignani, E., Torresan, S., Pasini, S., Critto, A., Marcomini, A., 2012. Climate change impact assessment in Veneto and Friuli plain groundwater. Part I: an integrate modeling approach for hazard scenario construction. Sci. Total Environ. 440, 154–166.
Bassi, G., 1972. Indagine sulle risorse idriche sotterranee della pianura alluvionale della Valle dell'Esino da Serra S. Quirico al mare. Officine Grafiche Calderini, p. 119.
Bates, B., Kundzewicz, Z.W., Wu, S., Palutikof, J.P., 2008. Climate change and water. Technical Paper VI of the Intergovernmental Panel on Climate Change. Intergovernmental Panel on Climate Change Secretariat, Geneva, p. 210.
Bear, J., Cheng, A., Sorek, S., Herrera, I., Ouazar, D., 1999. Seawater intrusion in coastal aquifers; concept, methods and practices. Kluwer Academic Publishers, p. 625.
Biondi, E., Baldoni, M., 1993. A bioclimatic characteristic of Italian Peninsula, atti del convegno "Effect atmospheric pollutants on climate and vegetation", Taormina, 26–28. GEA, pp. 225–250.
Biondi, E.I., Vagge, M., Baldoni, M., Taffetani, F., 2003. Biodiversità fitocenotica e paesaggistica dei fiumi dell'Italia centro-settentrionale: aspetti fitosociologici e sinfitosociologici. Studi Trent. Sci. Nat. Acta Biol. 80, 13–21.
Bordi, I.S., Frigio, P., Parenti, A., Speranza, A., Sutera, A., 2001. The analysis of the Standardized Precipitation Index in the Mediterranean area: regional patterns. Ann. Geophys. 44, 5–6.
Bucchignani, E., Gualdi, S., 2011. Gli scenari di cambiamento climatico. Il progetto TRUST -Life+ Tool per regional-scale assessment of groundwater storage improvement in adaptation to climate change. Autorità di bacino dei fiumi dell'Alto Adriatico, Venezia.
Calderoni, G., Cilla, G., Dramis, F., Gobbi, C., 2007. Environmental changes and human settlement in the central marches (Italy) during the early–middle Holocene. Physio-Géo. Géogr. Phys. Environ. 1, 21–32.
Carneiro, J.F., Boughriba, M., Correia, A., Zarhloule, Y., Rimi, A., El Houadi, B., 2010. Evaluation of climate change effects in a coastal aquifer in Morocco using a density-dependent numerical model. Environ. Earth Sci. 61 (2), 241–252.

Cattiaux, J., Douville, H., Peings, Y., 2013. European temperatures in CMIP5: origins of present-day biases and future uncertainties. Clim. Dyn. 1–19 http://dx.doi.org/10.1007/s00382-013-1731-y.
Clarke, D., Sanitwong, S., Ayutthaya, N., 2010. Predicted effects of climate change, vegetation and tree cover on dune slack habitats at Ainsdale on the Sefton Coast, UK. J. Coast. Conserv. 14 (2), 115–125.
Coltori, M., 1997. Human impact in the Holocene fluvial and coastal evolution of the Marche region, Central Italy. Catena 30 (4), 311–335.
Cotecchia, V., Grassi, D., Polemio, M., 2005. Carbonate aquifers in Apulia and seawater intrusion. Giornale Geol. Appl. (Ital. J. Eng. Geol.) 1, 219–231.
Crozier, M., Glade, T., 2005. Landslide hazard and risk: issues, concepts and approach. In: Glade, T., Anderson, M., Crozier, M. (Eds.), Landslide Hazard and Risk, Chichester. John Wiley & Sons, LtD, pp. 1–40.
Dams, J., Salvadore, E., Van Daele, T., Ntegeka, V., Willems, P., Batelaan, O., 2012. Spatio-temporal impact of climate change on the groundwater system. Hydrol. Earth Syst. Sci. 16, 1517–1531.
Dentoni, M., Deidda, R., Paniconi, C., Marrocu, M., Lecca, G., 2014. Seawater intrusion risk analysis under climate change conditions for the Gaza Strip aquifer (Palestine). EGU General Assembly. Copernicus.
DPR, 1988. Decree of the President of the Republic n. 236, 24 May 1988. Application of the European directive 80/778/CEE concerning the quality of water for human use.
Dragoni, W., Sukhija, B.S., 2008. Climate change and groundwater: a short review. Geol. Soc. Lond., Spec. Publ. 288 (1), 1–12.
EC, 2000. Water Framework Directive — 2000/60/EC.
EC, 2006. Groudwater Framework Directive — 2006/118/EC.
ESRI Inc., 1995. Understanding GIS: arc/info method. Geo-Information Intl.
Essink, G.H.P.O., Van Baaren, E.S., De Louw, P.G.B., 2010. Effects of climate change on coastal groundwater systems: a modeling study in the Netherlands. Water Resour. Res. 46, W00F04. http://dx.doi.org/10.1029/2009WR008719.
Ferguson, G., Gleeson, T., 2012. Vulnerability of coastal aquifers to groundwater use and climate change. Nat. Clim. Chang. 2, 342–345. http://dx.doi.org/10.1038/nclimate1413.
Fichefet, T., Morales Maqueda, M.A., 1999. Modelling the influence of snow accumulation and snow ice formation on the seasonal cycle of the Antarctic sea-ice cover. Clim. Dyn. 15, 251–268.
Franssen, H.J.H., 2009. The impact of climate change on groundwater resources. Int. J. Clim. Chang Strateg. Manag. 1 (3), 241–254.
Gemitzi, A., Stefanopoulos, K., 2011. Evaluation of the effects of climate and man intervention on groundwaters and their dependent ecosystems using time series analysis. J. Hydrol. 403 (1), 130–140.
Giambastiani, B.M.S., Antonellini, M., Oude Essink, G.H.P., Stuurman, R.J., 2007. Saltwater intrusion in the unconfined coastal aquifer of Ravenna (Italy): a numerical model. J. Hydrol. 340, 91–104.
Grassi, S., Netti, R., 2000. Sea water intrusion and mercury pollution of some coastal aquifers in the province of Grosseto (southern Tuscany—Italy). J. Hydrol. 237, 198–211.
Herrera-Pantoja, M., Hiscock, K., 2008. The effects of climate change on potential groundwater recharge in Great Britain. Hydrol. Process. 22, 73–86. http://dx.doi.org/10.1002/hyp.6620.
Holman, I.P., 2006. Climate change impacts on groundwater recharge uncertainty, shortcomings, and the way forward? Hydrogeol. J. 14, 637–647.
IPCC, 2007a. The physical science basis. Summary for Policymakers Contribution of Working Group I to the Fourth Assessment Report of the Intergovernmental Panel on Climate Change, Geneva.
IPCC, 2007b. Climate change 2007: impacts, adaptation and vulnerability. In: Parry, M.L., Canziani, O.F., Palutikof, J.P., van der Linden, P.J., Hanson, C.E. (Eds.), Contribution of Working Group II to the Fourth Assessment Report of the Intergovernmental Panel on Climate Change. Cambridge University Press, Cambridge, p. 976.
IPCC, 2014. The physical science basis. Working Group I contribution to the Fourth Assessment Report of the Intergovernmental Panel on Climate Change. Cambridge University Press, Cambridge.
Jyrkama, M.I., Sykes, J.F., 2007. The impact of climate change on spatially varying groundwater recharge in the Grand River watershed (Ontario). J. Hydrol. 338 (34), 237–250.
Kharin, V.V., Zwiers, F.W., Zhang, X., Wehner, M., 2013. Changes in temperature and precipitation extremes in the CMIP5 ensemble. Clim. Chang. 119 (2), 345–357.
Kløve, B., Ala-aho, P., Bertrand, G., Boukalova, Z., Ertürk, A., Goldscheider, N., Ilmonena, J., Karakayag, N., Kupfersbergerh, H., Kvœrnerb, J., Lundbergi, A., Mileusnićj, M., Moszczynskak, A., Muotkaa, T., Predal, E., Rossia, P., Siergieievi, D., Šimekd, J., Wachniewm, P., Anghelutal, V., Widerlundi, A., 2011. Groundwater dependent ecosystems. Part I: hydroecological status and trends. Environ. Sci. Pol. 14 (7), 770–781.
Landis, W.G., 2005. Regional scale ecological risk assessment, using the relative risk model, (ed) Landis WG CRC PRESS.
Madec, G., Delecluse, P., Imbard, M., Lévy, C., 1998. OPA 8.1 Ocean General Circulation Model reference manual. Note du Pôle de modélisation 11. Institut Pierre-Simon Laplace, p. 91.
Moore, W.S., 1996. Large groundwater inputs to coastal waters revealed by ^{226}Ra enrichments. Nature 380, 612–614.
Nakićenović, N., Alcamo, J., Davis, G., de Vries, H.J.M., Fenhann, J., Gaffin, S., Gregory, K., Grubler, A., Jung, T.Y., Kram, T., La Rovere, E.L., Michaelis, L., Mori, S., Morita, T., Papper, W., Pitcher, H., Price, L., Riahi, K., Roehrl, A., Rogner, H.-H., Sankovski, A., Schlesinger, M., Shukla, P., Smith, S., Swart, R., van Rooijen, S., Victor, N., Dadi, Z., 2000. Special Report on Emissions Scenarios. Intergovernmental Panel on Climate Change. Cambridge University Press, Cambridge.
Nanni, T., 1985. Le faide di subalveo delle Marche: inquadramento idrogeologico, qualità delle acque (ed) elementi di neotettonica. Materiali per la programmazione 2. Regione Marche, Ancona.

Post, V.E.A., 2005. Fresh and saline groundwater interaction in coastal aquifers: is our technology ready for the problems ahead? Hydrogeol. J. 13 (1), 120–123.

Post, V., Abarca, E., 2010. Preface: saltwater and freshwater interactions in coastal Aquifers. Hydrogeol. J. 18 (1), 1–4.

Praveena, S.M., Aris, A.Z., 2010. Groundwater resources assessment using numerical model: a case study in low-lying coastal area. Int. J. Environ. Sci. Technol. 7 (1), 135–146.

Ranjan, P., Kazama, S., Sawamoto, M., 2006. Effects of climate change on coastal fresh groundwater resources. Glob. Environ. Chang. 16 (4), 388–399.

Rasmussen, P., Sonnenborg, T.O., Goncear, G., Hinsby, K., 2013. Assessing impacts of climate change, sea level rise, and drainage canals on saltwater intrusion to coastal aquifer. Hydrol. Earth Syst. Sci. 17, 421–443. http://dx.doi.org/10.5194/hess-17-421-2013.

Re, V., Zuppi, G.M., 2011. Influence of precipitation and deep saline groundwater on the hydrological systems of Mediterranean coastal plains: a general overview. Hydrol. Sci. J. 56 (6), 966–980.

Rockel, B., Will, A., Hense, A., 2008. Special issue regional climate modelling with COSMO-CLM (CCLM). Meteorol. Z. 17.

Roeckner, E., Bäuml, G., Bonaventura, L., Brokopf, L., Esch, M., Giorgetta, M., Hagemann, S., Kirchner, I., Kornblueh, L., Manzini, E., Rhodin, A., Schlese, U., Schluzweida, U., Tompkins, A., 2003. The atmospheric GCM ECHAM-5. Max Planck Institut fuer Meteorologie Report N 349 (Hamburge, 140, ISSN 0937 1060).

Scibek, J., Allen, D.M., 2006. Comparing modelled responses of two high-permeability, unconfined aquifers to predicted climate change. Glob. Planet. Chang. 50 (1), 50–62.

Sherif, M.M., Singh, V.P., 1999. Effect of climate change on seawater intrusion in coastal aquifers. Hydrol. Process. 13 (8), 1277–1287.

Taylor, R.G., Scanlon, B., Döll, P., Rodell, M., van Beek, R., Wada, Y., Longuevergne, L., Leblanc, M., Famiglietti, J.S., Edmunds, M., Konikow, L., Green, T.R., Chen, J.,

Taniguchi, M., Bierkens, M.F.P., MacDonald, A., Fan, Y., Maxwell, R.M., Yechieli, Y., Gurdak, J.J., Allen, D., Shamsudduha, M., Hiscock, K., Yeh, P.J.F., Holman, I., Treidel, H., 2012. Ground water and climate change. Nat. Clim. Chang. http://dx.doi.org/10.1038/nclimate1744.

Torresan, S., Critto, A., Rizzi, J., Marcomini, A., 2012. Assessment of coastal vulnerability to climate change hazards at the regional scale: the case study of the North Adriatic sea. Nat. Hazard Earth Syst. Sci. 12, 1–22. http://dx.doi.org/10.5194/nhess-12-1-2012.

UKCIP, 2003. Climate adaptation: risk, uncertainty and decision-making. In: Willows, Robert, Connell, Richenda (Eds.), (166 pp.).

UNEP, 2009. Ecosystem management programme. A new approach to sustainability. http://www.unep.org/ecosystemmanagement/LinkClick.aspx?fileticket=gbPVsoUCp-E%3D&tabid=311&mid=670 (accessed 13 June 2013).

Werner, A.D., 2010. A review of seawater intrusion and its management in Australia. Hydrogeol. J. 18 (1), 281–285.

Werner, A.D., Bakker, M., Post, V.E.A., Vandenbohede, A., Lu, C., Ataie-Ashtiani, B., Simmons, C.T., Barry, D.A., 2012. Seawater intrusion processes, investigation and management: recent advances and future challenges. Adv. Water Resour. 51, 3–26.

Wilby, R.L, Troni, J., Biot, Y., Tedd, L, Hewitson, B.C, Smithe, D.M., Suttonf, R.T., 2009. A review of climate risk information for adaptation and development planning. Int. J. Climatol. 29, 1193–1215.

Web References

http://www.lifesalt.it/en/idea.html (Accessed: 25 June, 2012).

http://www.cmcc.it (Accessed 20 June, 2012).

http://www.eea.europa.eu/publications/COR0-landcover (Accessed 15 June, 2012).

http://www.cbd.int/ecosystem/ (last accessed: 4 November, 2012).